

PREDICTING THE PERFORMANCES OF COHERENT ELECTRON COOLING WITH PLASMA CASCADE AMPLIFIER*

G. Wang[#], V. N. Litvinenko and J. Ma, BNL, Upton, NY, USA

Abstract

Recently, we proposed a new type of instability, Plasma Cascade Instability (PCI), to be used as the amplification mechanism of a Coherent Electron Cooling (CeC) system, which we call Plasma Cascade Amplifier (PCA). In this work, we present our analytical estimate of the cooling force as expected from a PCA-based CeC system. As an example, we apply our analysis to a planned PCA-based CeC test system and investigate the evolution of the circulating ion bunch in the presence of cooling.

INTRODUCTION

Cooling high energy, high intensity hadron beams remains one of the serious challenges in modern accelerator physics. Such cooling of natural emittances, while overcoming and mitigating other limitations, guarantees longer, more efficient stores that would result in significantly higher integrated luminosity in a hadron collider such as the Large Hadron Collider (LHC) at CERN, the Relativistic Heavy Ion Collider (RHIC) at the Brookhaven National Laboratory (BNL) or a future Electron-Ion Collider (EIC). One of the candidates to provide effective cooling for a high luminosity EIC is Coherent electron Cooling (CeC)[1]. CeC belongs to the family of stochastic coolers, but with the amplifier's bandwidth extending into the optical region, e.g. beyond the THz range. Several possible broadband CeC amplifier, based on instabilities in the electron beam, have been suggested including high-gain free-electron lasers (FEL), microbunching instability (MBI) [2-4] and the plasma cascade instability (PCI) [5].

In this work, we have developed an analytical tool to estimate the performance of the plasma-cascade amplifier (PCA) based CeC system. Section II shows our derivation of the electrons' line density modulation induced by a moving ion. In section III, we use the results in reference [5] to obtain the amplified line density perturbation with the initial condition derived in section II. From the amplified line density perturbation, we derived the longitudinal cooling field in section IV. We implement the one turn energy kick that ions receive from the cooling section into a tracking code and section V consists of our prediction for a test system of the PCA-based CeC.

LINE DENSITY MODULATION AT MODULATOR

Regardless of the amplification mechanism, a CeC system consists of a modulator, an amplifier and a kicker. To derive the longitudinal cooling force at the kicker section, we start with deriving electrons' line density modulation at the exit of the modulator. For a uniform electron beam with $\kappa-2$ velocity distribution, the 3-D density modulation in the wave-vector domain is given by[6]

$$\tilde{n}_1(\vec{k}, t) = \frac{Z_i \omega_p^2}{\omega_p^2 + \lambda(\vec{k})^2} \left[1 - e^{\lambda(\vec{k})t} \left(\cos(\omega_p t) - \frac{\lambda(\vec{k})}{\omega_p} \sin(\omega_p t) \right) \right], \quad (1)$$

where ω_p is the angular plasma frequency in the co-moving frame, \vec{k} is the wave vector, Z_i is the charge number of the ion, \vec{v}_0 is the velocity of the ion, β_x , β_y , and β_z are the velocity spread of electrons, and

$$\lambda(\vec{k}) = i\vec{k} \cdot \vec{v}_0 - \sqrt{(k_x \beta_x)^2 + (k_y \beta_y)^2 + (k_z \beta_z)^2}. \quad (2)$$

The line number density modulation in the longitudinal wave vector, k_z , domain is given by $\tilde{n}_1(0, 0, k_z, t)$, i.e.

$$\tilde{\rho}_1(k_z) = \frac{Z_i e}{1 + \bar{\lambda}_z(k_z)^2} \left[1 - e^{\bar{\lambda}_z(k_z) \psi_m} (\cos \psi_m - \bar{\lambda}_z(k_z) \sin \psi_m) \right], \quad (3)$$

where $\bar{\lambda}_z(k_z) = (ik_z v_{0z} - |k_z| \beta_z) / \omega_p$, $\psi_m = 2\pi L_m / \lambda_{p,lab}$ is the phase advance of plasma oscillation in the modulator, L_m is the length of the modulator section and $\lambda_{p,lab}$ is the plasma wavelength in the lab frame. The line number density in space-time domain is given by the inverse Fourier transformation of Eq. (3):

$$\begin{aligned} \rho_{1z}(z) &= \frac{1}{2\pi} \int_{-\infty}^{\infty} e^{ik_z z} \tilde{\rho}_1(k_z) dk_z \\ &= \frac{Z_i e}{\pi a_z} \int_0^{\psi_m} \frac{\tau \sin \tau}{\left(\frac{z}{a_z} + \frac{v_{0z}}{\beta_z} \tau \right)^2 + \tau^2} d\tau \end{aligned}, \quad (4)$$

with $a_z = \beta_z / \omega_p$ being the longitudinal Debye length in the co-moving frame.

AMPLIFICATION OF LINE DENSITY MODULATION IN PCA

For the electrons with uniform spatial and Lorentzian energy distribution, the evolution of their line density distribution in PCA is determined by the following expression[5]:

* Work supported by Brookhaven Science Associates, LLC under Contract No. DE-AC02-98CH10886 with the U.S. Department of Energy.
[#]gawang@bnl.gov

$$\tilde{\rho}_{2,\text{inf}}(k_z) = g_{\text{amp}} \exp\left(-|k_z| \beta_z \frac{L_{\text{amp}}}{\gamma c}\right) \tilde{\rho}_1(k_z), \quad (5)$$

where g_{amp} is the gain from PCA for an electron beam with zero energy spread and the exponential factor is the reduction of gain due to energy spread, i.e. Landau damping. For a transversely finite electron beam with radius of a_{amp} and beer-can distribution, the longitudinal space charge field induced by line density modulation is reduced by the following factor [7, 8]:

$$R_{\text{amp}}(k_z) = k_z^2 a_{\text{amp}}^2 \int_0^1 \eta K_0(|k_z| a_{\text{amp}} \cdot \eta) d\eta, \quad (6)$$

which will also reduce the PCA gain. Figure 1 plots the reduction factor of the on-axis longitudinal space charge field due to finite transverse size as a function of the longitudinal wave number, k_z .

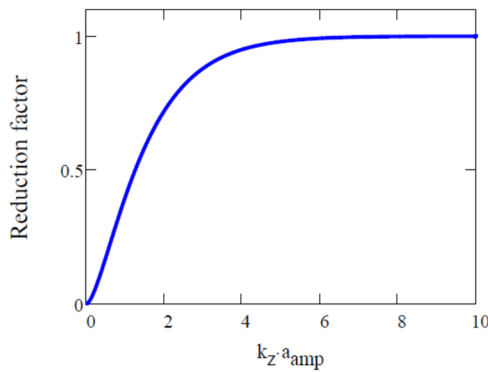


Figure 1: Reduction factor of longitudinal space charge field with finite transverse size. The abscissa is $k_z a_{\text{amp}}$ and the ordinate is the ratio of the on-axis longitudinal space charge field generated by a sinusoidal line density modulation with finite transverse size and that with infinite transverse size.

If we assume that the PCA gain is reduced by the same factor as the longitudinal space charge field, the amplified line density modulation for a transversely finite beam becomes

$$\tilde{\rho}_2(k_z) = g_{\text{amp}} R_{\text{amp}}(k_z) \exp\left(-|k_z| \beta_z \frac{L_{\text{amp}}}{\gamma c}\right) \tilde{\rho}_1(k_z). \quad (7)$$

As shown in Fig. 2, Landau damping due to energy spread of the electrons limits the amplification gain for short wavelength components and the transverse size of the electron beam significantly reduces the gain at long wavelength. The space-time domain line density perturbation after PCA amplification is given by the inverse Fourier transformation of Eq. (7):

$$\rho_2(z) = \frac{1}{2\pi} \int_{-\infty}^{\infty} \tilde{\rho}_2(k_z) e^{ik_z z} dk_z. \quad (8)$$

Figure 3 shows how the line density perturbation after PCA amplification. It is worth noting that for an infinitely wide electron beam the line density perturbation is always positive. However, after including the reduction factor due to finite transverse size of the electron beam, the

density modulation has both positive and negative values and the total number of electrons is conserved since $\tilde{\rho}_2(k_z)$ vanishes at $k_z = 0$.

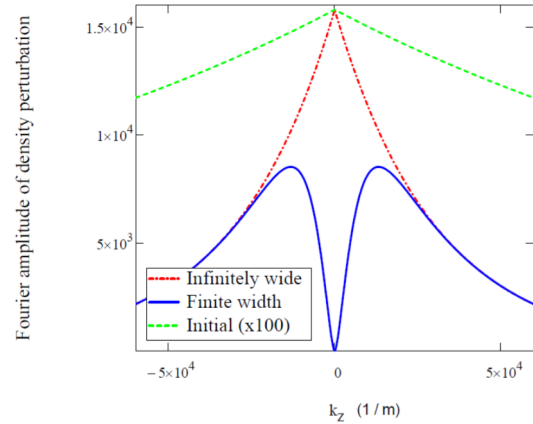


Figure 2: Fourier components of the amplified line density by PCA with parameters taken from Table 1. The abscissa is the longitudinal wave vector in co-moving frame. The green line is the initial line density modulation before amplification as calculated from Eq. (3) (multiplied by 100 for visibility); the red curve is the amplified line density modulation for an infinitely wide beam as calculated from Eq. (5); and the blue curve is the amplified line density modulation for electron beam with finite width as calculated from Eq. (7).

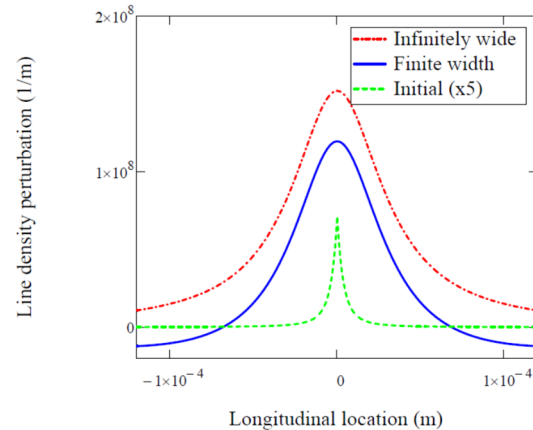


Figure 3: The amplified line density perturbation by PCA with parameters taken from Table 1. The green dash line is the initial line density modulation before amplification (multiplied by 5 for visibility); the red dash-dot curve is the amplified line density modulation for an infinitely wide beam; and the blue solid curve is the amplified line density modulation for electron beam with finite width. Parameters in Table 1 are used in generating the plots.

LONGITUDINAL ELECTRIC FIELD IN THE KICKER

The longitudinal electric field induced by the line density perturbation, $\rho_2(z)$, is determined by the Poisson equation:

$$\frac{1}{r} \left[\frac{\partial}{\partial r} \left(r \frac{\partial}{\partial r} \varphi(r, z) \right) \right] + \frac{\partial^2}{\partial z^2} \varphi(r, z) = \frac{1}{\varepsilon_0} \rho_2(z) f_{\perp}(r), \quad (9)$$

where $\varphi(r, z)$ is the electric potential and $f_{\perp}(r)$ is the transverse distribution of the electron beam. For beer-can distribution, the transverse distribution function is

$$f_{\perp}(r) = \frac{1}{\pi a^2} H(a - r), \quad (10)$$

with $H(x)$ being the Heaviside step function. Inserting Eq. (10) into Eq. (9) and solving the resulting differential equation yields

$$E_z(r, z) = -\frac{\partial \varphi}{\partial z} = \frac{1}{2\pi} \int_{-\infty}^{\infty} \tilde{E}_z(r, k_z) e^{ik_z z} dk_z, \quad (11)$$

with

$$\tilde{E}_z(r) = -ik_z \frac{\tilde{\rho}_2(k_z)}{\pi \varepsilon_0} \times \quad (12)$$

$$\left[I_0(k_z r) \int_{r/a}^1 \eta K_0(k_z a \cdot \eta) d\eta + K_0(k_z r) \int_0^{r/a} \eta I_0(k_z a \cdot \eta) d\eta \right]$$

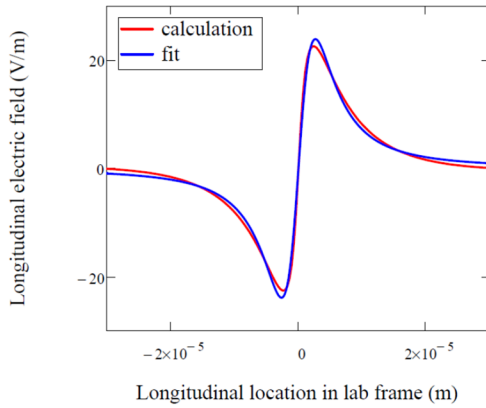


Figure 4: The longitudinal cooling field in the kicker section of the PCA-based CeC system with parameters listed in Table 1. The red curve is calculated from Eq. (11) and the blue curve is generated from the fitting formula Eq. (13) with $E_0 = 62V/m$ and $\sigma_c = 3.75\mu m$.

In practice, the results of Eq. (11) can be fitted by the formula

$$E_{fit}(z) = E_0 \cdot \frac{z}{\sigma_c} \left[1 + \frac{z^2}{\sigma_c^2} \right]^{-3/2}, \quad (13)$$

with reasonable accuracy as shown in Fig. 4 and Eq. (13) is usually more convenient to be implemented into a tracking code to simulate the circulating ion bunch.

EVOLUTION OF ION BUNCH PROFILE

Using Eq. (13), the energy kick (normalized to the rest energy of the ion, i.e. $A_i m_u c^2$) received by the j^{th} ion on its N^{th} circulation is [9]

$$\Delta\gamma_{j,N} = -g_{\gamma} \frac{(D \cdot \delta_{j,N})}{\sigma_c} \left[1 + \frac{(D \cdot \delta_{j,N})^2}{\sigma_c^2} \right]^{-3/2} + g_{\gamma} \sqrt{\frac{3\pi}{8} \rho_{ion}(z_{j,N}) \sigma_c} \cdot X_{j,N} + \frac{g_{\gamma}}{Z_i} \sqrt{\frac{3\pi}{8} \rho_e(z_{j,N}) \sigma_c} \cdot Y_{j,N} \quad (14)$$

where $\delta_{j,N}$ is the relative energy deviation of the ion, ρ_{ion} and ρ_e is the line density of the ions and electrons at the location of the j^{th} ion, $g_{\gamma} = Z_i e E_0 L_k / (A_i m_u c^2)$, σ_c and E_0 are fitting parameters to be determined from eqs. (11) and (13), $X_{j,N}$ and $Y_{j,N}$ are random numbers uniformly distributed between -1 and 1, D is the longitudinal dispersion of the electrons (also called R_{56}) and L_k is the length of the kicker section. Eq. (14) is implemented into a tracking code to predict the profile of an ion bunch. The code also includes longitudinal IBS effects, which, in the absence of the cooling, causes the bunch length to grow as shown in fig. 5 (red). Figure 5 also shows that, according to our estimates, the peak current of the cooled bunch will be higher than the witness bunch by $\sim 70\%$.

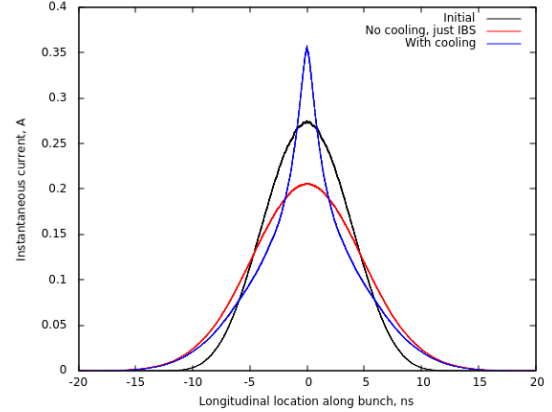


Figure 5: The longitudinal profile of the ion bunch after 40 minutes of cooling. The black curve shows the initial bunch longitudinal profile with 2×10^8 Au ion and 3.55 ns of bunch length. The blue curve shows the ion bunch profile after cooling and the red curve shows a witness ion bunch not interacting with electron bunch.

Table 1: Parameters for PCA-based CeC test at BNL

e beam energy, γ	28.5	e peak current	100 A
e beam size at modulator/kicker	0.94 mm	Energy spread, rms	10^{-4}
e bunch length	15 ps	Beam waist at PCA, a_{amp}	0.2 mm
Modulator length, L_m	3 m	Kicker length, L_k	3 m
PCA length (4 cells)	8 m	Ion charge number, Z_i	79
PCA gain	100	Ion mass number, A_i	197

REFERENCES

- [1] V. N. Litvinenko, Y. S. Derbenev, *Physical Review Letters*, 102 (2009) 114801.
- [2] D. Ratner, *Physical Review Letters*, 111 (2013) 084802.
- [3] G. Stupakov, *Physical Review Accelerators and Beams*, 21 (2018) 114402.
- [4] G. Stupakov, P. Baxevanis, *Physical Review Accelerators and Beams*, 22 (2019) 034401.

- [5] V. Litvinenko, G. Wang, D. Kayran, Y. Jing, J. Ma, I. Pinayev, arXiv preprint arXiv:1802.08677, (2018).
- [6] G. Wang, M. Blaskiewicz, Phys. Rev. E, 78 (2008) 026413.
- [7] G. Stupakov, M. Zolotarev, in *Proc. FEL'13*, New York, USA, 2013, pp. 132-135.
- [8] V. N. Litvinenko, in *Proc. COOL'13*, Murren, Switzerland, 2013, pp. 175.
- [9] G. Wang, M. Blaskiewicz, V. Litvinenko, in *Proc. 7th International Particle Accelerator Conference (IPAC'16)*, Busan, Korea, May 8-13, 2016, pp. 1243-1246.